Structural characteristics of foam-insulated diaphragm panels

K. G. GEBREMEDHIN and J. A. BARTSCH

Agricultural and Biological Engineering Department, Cornell University, Ithica, N.Y. 14853. *Received 7 August 1987, accepted 28 April 1988.*

Gebremedhin, K. G. and Bartsch, J. A. 1988. **Structural characteristics of foam-insulated diaphragm panels**: Can. Agric. Eng. 30: 299–306. Load-deflection characteristics and failure modes of urethane-foam-insulated, metal-clad, timber-framed and screw-fastened ceiling diaphragms are presented. Eight diaphragms, 2.44 m × 6.10 m, were built and tested as deep beams and another eight diaphragms, 2.44 m × 3.66 m, were tested as short cantilever beams, primarily in shear. In-plane loads were applied to simulate wind loads carried by ceilings of farm buildings. Major variables include type of skin (steel versus aluminum), presence of foam (urethane foamed versus unfoamed panels), and density of urethane foam (32 and 48 kg/m³). The results are useful in incorporating diaphragm or stressed-skin principles into urethane foam insulated ceilings or walls of post or stud-wall building designs.

INTRODUCTION

Besides providing high thermal insulation, urethane foam insulated diaphragms are also efficient (high strength to weight ratio) structural members. The metal skin acts in combination with the foam to resist external bending loads such as wind or roof loads.

The urethane foam is neither uniform nor isotropic. Therefore, structural properties of composite diaphragms must be derived from full-scale load tests. The strength of the foam part is affected by the type of foam, the density of the foam, and the foaming process. There is no current standard for specifying foam properties.

The purpose of this study is to determine the structural characteristics and failure modes of foamed-in-place metal-skin ceilings with timber framing for use as shear diaphragms in agricultural buildings. These types of diaphragms are commonly used for ceiling and wall systems of environmentally controlled fruit and vegetable storage facilities.

Prototype ceiling diaphragms were tested as deep beams (Fig. 1a) and as cantilever-type (Fig. 1b) to determine their load-deflection characteristics and failure modes. A total of 16 separate experiments (eight deep beam tests and eight cantilever-type tests) were conducted. The information from these tests supplements earlier published data for non-insulated ceiling diaphragms (Gebremedhin and Irish 1986), and work done by Turnbull et al. (1982, 1985) on steel roof diaphragms for wind bracing in agricultural buildings.

TEST PROCEDURE AND APPARATUS

Framing

Framing consisted of 38 mm × 89 mm (2 × 4) members simulating ceiling joists or lower chords of trusses 1.22 m o.c., and 38 mm × 89 mm edge beams nailed flat to the ends of the chords by 2-10 d nails. The chords were placed on edge and all lumber was construction grade Douglas-fir at ≤19% moisture content.

Metal skin

Steel and aluminum panels, 29-gage (0.368 mm) were used for the study. The profile of the panels consists of 19 mm deep major ribs 228 mm o.c. (Figure 1). Each panel covers 0.91 m of diaphragm width.

Fasteners

Metal-to-frame fasteners were 25 mm × 4.27 mm (No. 8) wood-grip, self drilling steel screws. Edge fasteners (along the long edges of the diaphragm) were placed on each side of major ribs as recommended by the manufacturer of the metal skin (detail in Fig. 1). End fasteners (along the end of the diaphragm) and interior fasteners (along the intermediate chords) were spaced 407 mm o.c. Sidelap stitch fasteners were 16 mm × 5.46 mm (No. 12) self-drilling and self-tapping steel screws spaced 203 mm o.c. These connectors pass only through the two lapped sheets to transfer shear from panel to panel.

Foam insulation

The cavity against the metal skin and between the chords was primed and foamed with urethane foam insulation according to standard industry practice. Foam densities of 32 and 48 kg/m³ were used, these being common for fruit and vegetable storage facilities. Both foam densities were used in the beam test but only the 48 kg/m³ density was used in the shear test. Foaming was done by a commercial urethane foam applicator.

Testing system

The study also included development of a testing and data acquisition system to determine diaphragm strength and stiffness. The system allowed testing of diaphragms both in bending and shear.

Testing diaphragms as deep beams. Eight diaphragms were tested as deep beams. In-plane loads simulating wind were applied by four identical, equally spaced hydraulic cylinders (Fig. 1a). The cylinders were connected by manifold to a single electronically modulated pressure control valve. The double acting cylinders were 76 mm bore by 203 mm throw. Rod-end type strain gage load cells were threaded onto the piston rods of the cylinders and fitted with ball-and-cup connections to the chords where the force was to be applied. The ball-and-cup connection allowed for minor changes in alignment as the forces were being applied and prevented damage to the load cells and cylinder pistol rods. Swivel plates were used at the fixed ends of the cylinders where they pushed against the supports.

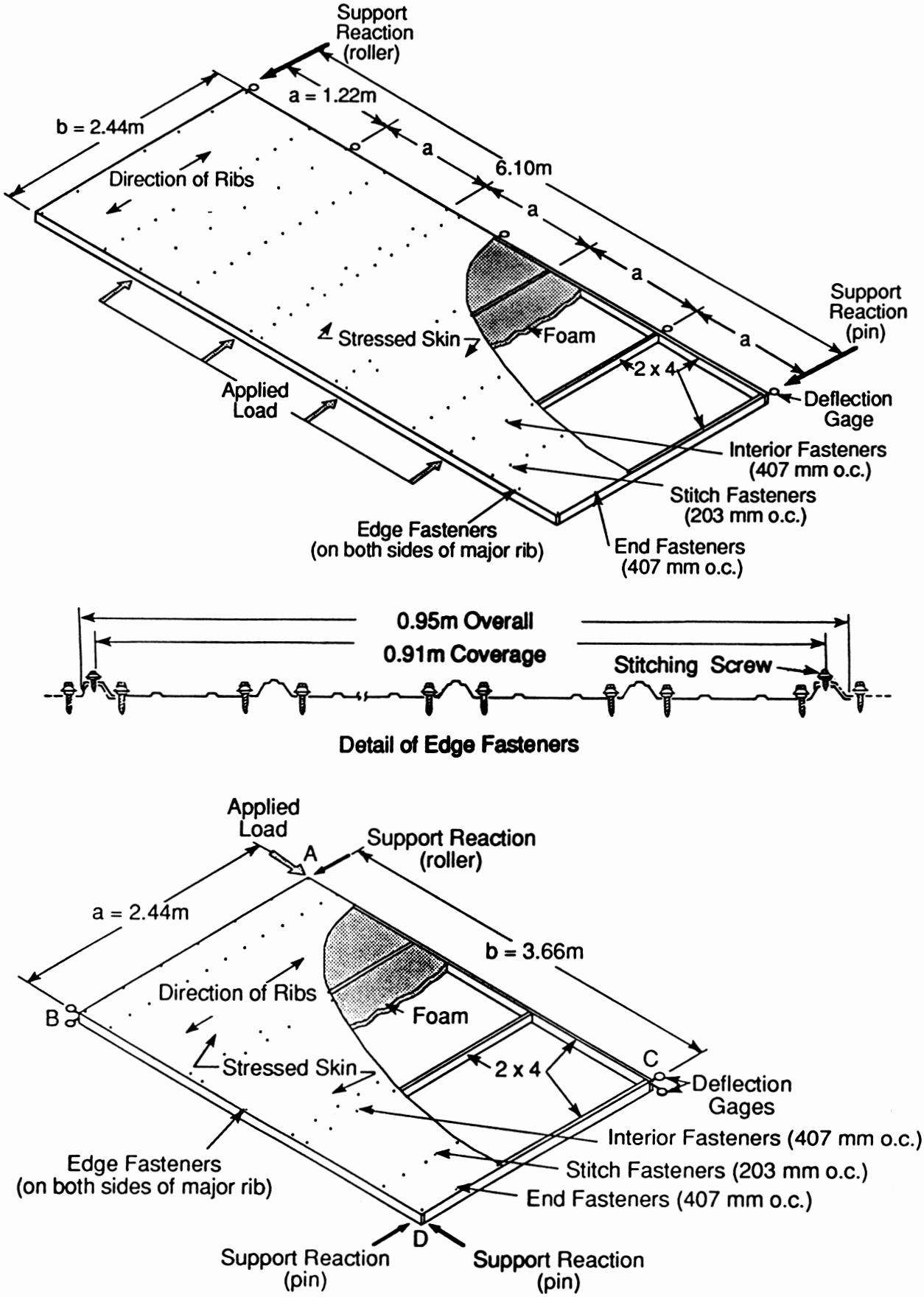

Figure 1. Diaphragm test setup (a) deep beam, (b) cantilever, and details.

Testing diaphragms as cantilever-type. For the shear tests, one cylinder was used when the applied force was less than or equal to 26.7 kN, and two cylinders were used in parallel with a whiffle-tree connection when the force required exceeded 26.7 kN. This force limitation equalled the maximum load capacity of the transducers.

In the shear tests, the cylinders were reversed such that the ball-and-cup connections were at the support and the fixed ends of the cylinders were pinned to a whiffle-tree. The whiffle-tree was pinned at a single point to a carrier link which was attached to the corner of the diaphragm being tested. This arrangement allowed the combined use of two cylinders in "parallel" to exert a single point force on the diaphragm.

The cylinders were connected to a manifold using flexible 6-mm internal diameter thermoplastic hose with quick-connect couplings. Various hydraulic devices were assembled on a plywood board, including a pressure relief valve, oil filter, pressure gages, directional control valve, needle valves, solenoid pressure control valves, and manifold connections for both pressure and return lines. Line pressure was supplied by a hydraulic pump. The directional control valve permitted reversing the action of the cylinders, and the needle valve allowed meeting the fluid flow for proper operation of the solenoid valve. The proportional solenoid pressure control valve was the "heart" of the system, permitting close control of the pressure in the cylinders and thereby the forces exerted by the cylinders. A schematic diagram of the assembly of the hydraulic devices and control system is shown in Fig. 2.

A data acquisition and control system was developed for monitoring and controlling the hydraulic pressures applied to the hydraulic cylinders. Strain gage load cell transducers with signal conditioning amplifiers provided 0 to 5 V dc signals linearly proportional to the forces exerted by the hydraulic cylinders. These signals were digitized, converted into corresponding force values, and then recorded. The analog force signal was used as the feed back control signal for controlling the applied forces during the tests. The applied force was determined by the magnitude of a 0- to 10-V dc proportional signal sent from the computer's digital-to-analog output module to the electronic controller which operated the proportional solenoid pressure control valve. The computer monitored the readings of the load cell and made adjustments in the control valve signal, which were proportional to the error in the force signal, in a feed-back arrangement to maintain the desired force. The pressure control valve regulated the hydraulic pressure on the cylinders, and therefore the force applied by the cylinders. This system had the capability of monitoring one to four load cells and could control two proportional solenoid valves simultaneously.

Control of load application during the testing process was conducted as follows: (1) the desired load was entered into the computer program, and (2) the program adjusted the line pressure to the hydraulic cylinders based on the discrepancy between the desired and measured loads. This continued until the difference between the applied and measured loads became negligible. A flow chart of the data acquisition and control system is shown in Fig. 3.

Loading procedure

All diaphragms were tested with the metal skin on top (ceiling upside-down) to better observe the effects of loading on the skin and fasteners. The loading procedure was:

(1) Apply an initial minimum line pressure to preload the diaphragm in the test stand and to set deflection gages to zero. Dial deflection gages, as located in Fig. 1a and 1b, indicate in-plane deflections. Deflections were manually recorded and then entered into the computer for analysis.

(2) Apply a load increment of 500 N every 2 min, record deflections and any structural behavior at each increment. Loads were applied in equal increments from zero to failure. The increment of loading was chosen so that sufficient number of readings are obtained to determine the load-deflection curve.

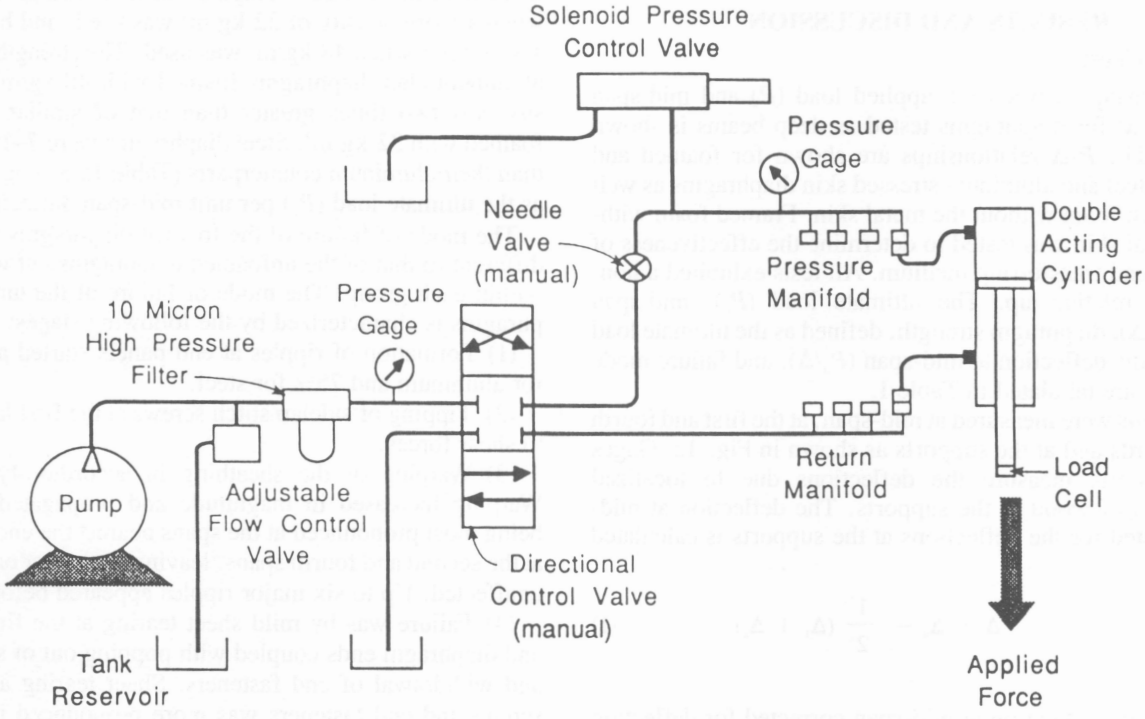

Figure 2. A schematic diagram of the hydraulic devices and control system assembly.

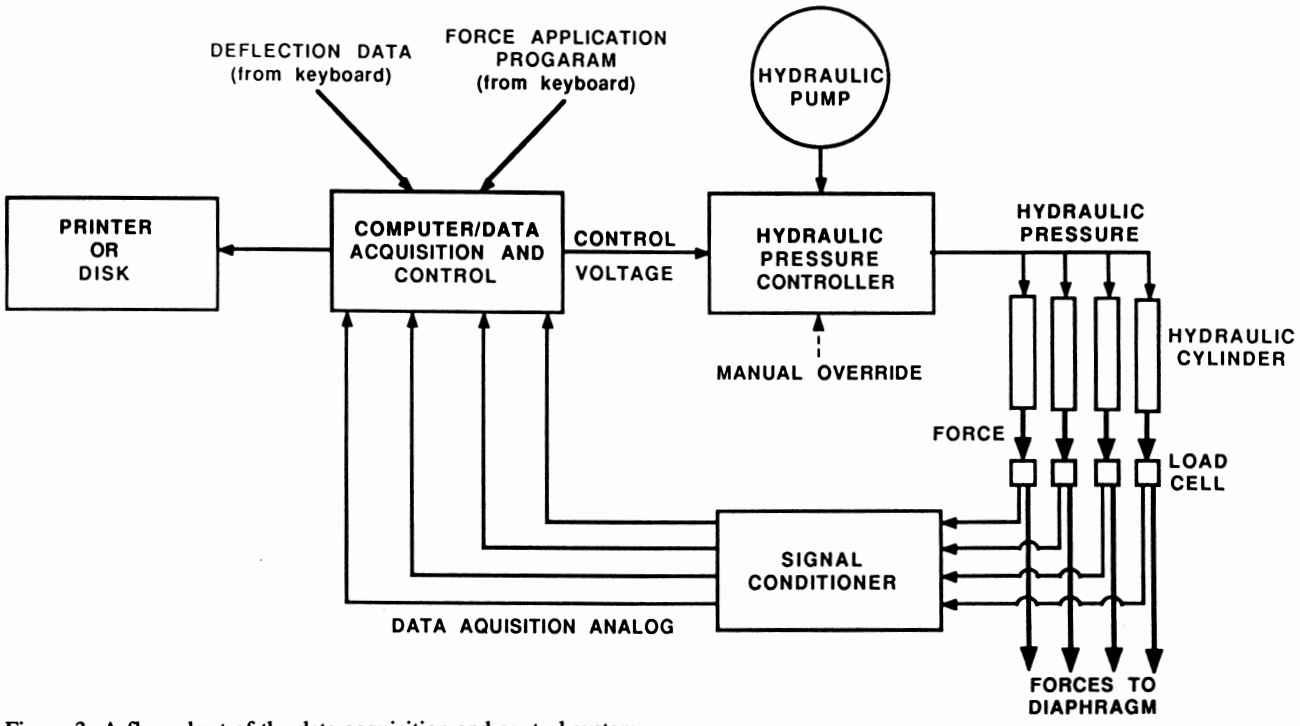

Figure 3. A flow chart of the data acquisition and control system.

This rate of load application was adequate to permit the structure to stabilize and allowed time to read and record data manually. The stepwise loading procedure does not affect the results other than for minor creep.

(3) Terminate loading when deflection increased with no detectable increase in load-cell readings or when permanent damage of any element of the diaphragm starts to occur.

The above procedures were followed when testing both the deep beam and cantilever-type tests.

RESULTS AND DISCUSSION

Deep Beam Tests

The relationship between the applied load (P) and mid-span deflection (Δ) for diaphragms tested as deep beams is shown in Fig. 4. The P-Δ relationships are shown for foamed and unfoamed steel and aluminum stressed skin diaphragms as well as for framed foam without the metal skin. Framed foam without the metal skin was tested to determine the effectiveness of foam as a load transferring medium. All tests exhibited a nonlinear P-Δ relationship. The ultimate load (P_u), mid-span deflection (Δ), diaphragm strength, defined as the ultimate load divided by the deflection at mid-span (P_u/Δ), and failure mode of each test are tabulated in Table I.

Deflections were measured at mid-span, at the first and fourth interior chords and at the supports as shown in Fig. 1a. Gages at the supports measure the deflections due to localized compression of wood at the supports. The deflection at mid-span corrected for the deflections at the supports is calculated as

$$\Delta = \Delta_u - \frac{1}{2}(\Delta_1 + \Delta_2) \qquad (1)$$

where:

Δ = deflection at mid-span corrected for deflection at the supports,

Δ_u = uncorrected deflection at mid-span,

Δ_1 and Δ_2 = deflections at the supports due to localized compression of wood.

The corrected deflection, Δ, consists of bending and shear deflections. The load-deflection curves in Fig. 4 are plotted using the corrected deflections.

Urethane foam combined with metal skin increases panel strength by providing more effective diaphragm action, i.e., transferring load by shear. Foaming increased the strength by more than three times compared to non-foamed diaphragms, when a foam density of 32 kg/m^3 was used, and by more than seven times when 48 kg/m^3 was used. The strength of steel- or aluminum-clad diaphragms foamed with 48 kg/m^3 foam density was two times greater than that of similar diaphragms foamed with 32 kg/m^3. Steel diaphragms were 7–19% stronger than their aluminum counterparts (Table I). Strength is defined as the ultimate load (P_u) per unit mid-span deflection (Δ).

The mode of failure of the foamed diaphragms was entirely different to that of the unfoamed diaphragms but was identical within each group. The mode of failure of the unfoamed diaphragms is characterized by the following stages:

(1) Formation of ripples at end panels started at 50% of P_u for aluminum and 75% for steel.

(2) Tipping of sidelap stitch screws at the first lap joints due to shear forces.

(3) Warping of the sheathing in accordion-type manner. Warping increased in magnitude and propagated with load, being most pronounced at the spans nearest the ends, moderate at the second and fourth spans, leaving the center one-fifth span unaffected. Up to six major ripples appeared before failure.

(4) Failure was by mild sheet tearing at the first lap joints and diaphragm ends coupled with popping out of stitch screws and withdrawal of end fasteners. Sheet tearing around stitch screws and end fasteners was more pronounced in aluminum than in steel.

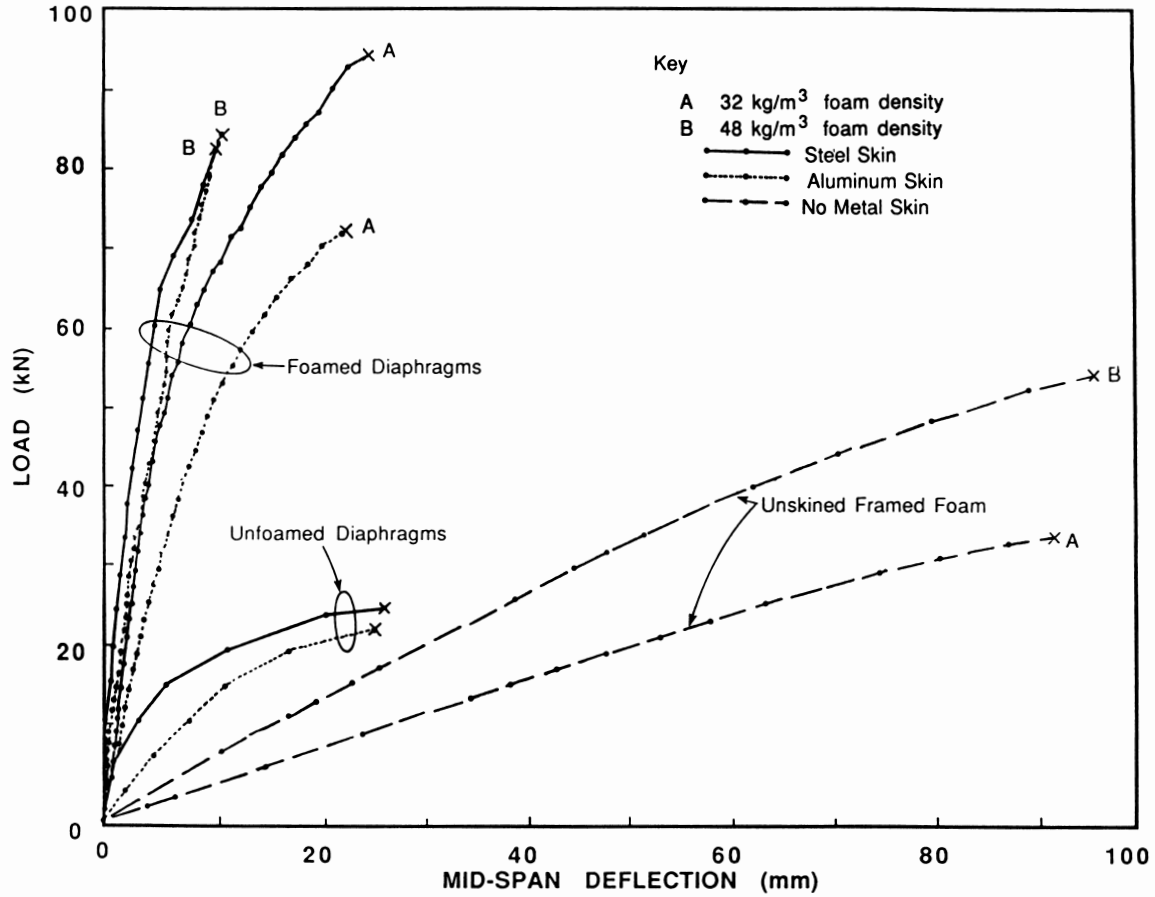

Figure 4. Load-deflection relationships for 2.44 m × 6.10-m diaphragms tested as deep beams.

The mode of failure of the foamed diaphragms, on the other hand, was sudden and dramatic. The metal skin showed no noticeable stress until a sudden and dramatic shear failure occurred at the first lap joint in the underlying foam. The shear failure was coupled with mild sheet tearing at the stitching screws but without rib buckling or any other deformation in the metal skin.

To determine the contribution of the foam as a shear transferring medium, duplicate pairs of framed foam panels (without the metal skin) were built and tested. The mid-span deflection of these systems was significantly larger than that of their skinned counterparts, thus greatly lowering their strength. The ultimate load, mid-span deflection and (P_u/Δ) values for these systems are given in Table I, and the P-Δ relationships are shown in Fig. 4. The results suggest that the foam alone (without the metal skin), besides being an impractical structural component, cannot provide sufficient diaphragm action. Besides, foam undergoes a significant degree of strain creep under a sustained long-term load (Ting 1986).

Shear tests

Diaphragm in-plane shear strength and stiffness can also be assessed by testing cantilever-type diaphragms, as shown in Fig. 1b. Various investigators used this testing method to determine strength and stiffness of prototype diaphragms (Luttrell 1967; White 1978; Hoagland and Bundy 1983). In all of the reports given by these investigators, shear strength is defined as the ultimate shear load per unit length, where the length of the diaphragm is measured parallel to the direction of the applied load.

The measured deflection at the free end of the cantilever beam diaphragm is influenced by deflections due to localized compression of wood at the supports. The deflection at the free end corrected for the deflections at the supports is calculated as

$$\Delta = \Delta_3 - \Delta_1 - \frac{a}{b}(\Delta_2 + \Delta_4) \qquad (2)$$

where:

Δ = deflection at the free end of the cantilever beam diaphragm corrected for the deflections at the supports.
Δ_1 = horizontal deflection due to localized compression of wood at the reaction support (measured at Corner B)
Δ_2 = vertical deflection of diaphragm at Corner B
Δ_3 = horizontal deflection of diaphragm at Corner C
Δ_4 = vertical deflection due to localized compression of wood at the reaction support (measured at Corner C)
a,b = dimensions of the test frame shown in Fig. 1a and 1b.

The four deflection values in Eq. 2 are measured with dial gages placed at the locations shown in Fig. 1b.

The corrected deflection, Δ, includes bending and shear deflections. The load-deflection curves in Fig. 5 are plotted using the measured deflections corrected for deflections at the supports.

A total of eight diaphragms were tested in shear mode. The results of the six tests are summarized in Table II and the load-

Table I. Load-deflection characteristics and failure modes of diaphragms tested as deep beams†

Type of sheathing	Foam density (kg/m³)	P_u (kN)	Δ (nm)	Strength (P_u/Δ) (kN/mm)	Failure mode
Steel	No foam	27.1	27	1.0	Sheet tearing at stitch screws and end fasteners
Steel	32	94.6	26	3.7	Shear in foam and sheet tearing at 1st sidelap joint
Steel	48	83.0	11	7.6	Shear in foam at 1st sidelap joint
Aluminum	No foam	24.5	26	0.9	Sheet tearing at stitch screws and end fasteners
Aluminum	32	73.3	24	3.1	Shear in foam and sheet tearing at 1st sidelap joint
Aluminum	48	84.6	12	7.1	Shear in foam and sheet tearing at 1st sidelap joint
No skin	32	37.2	95	0.4	Shear in foam at 1st span
No skin	48	57.7	96	0.6	Shear in foam at 1st span

†Diaphragms were 2.44 m × 6.10 m.

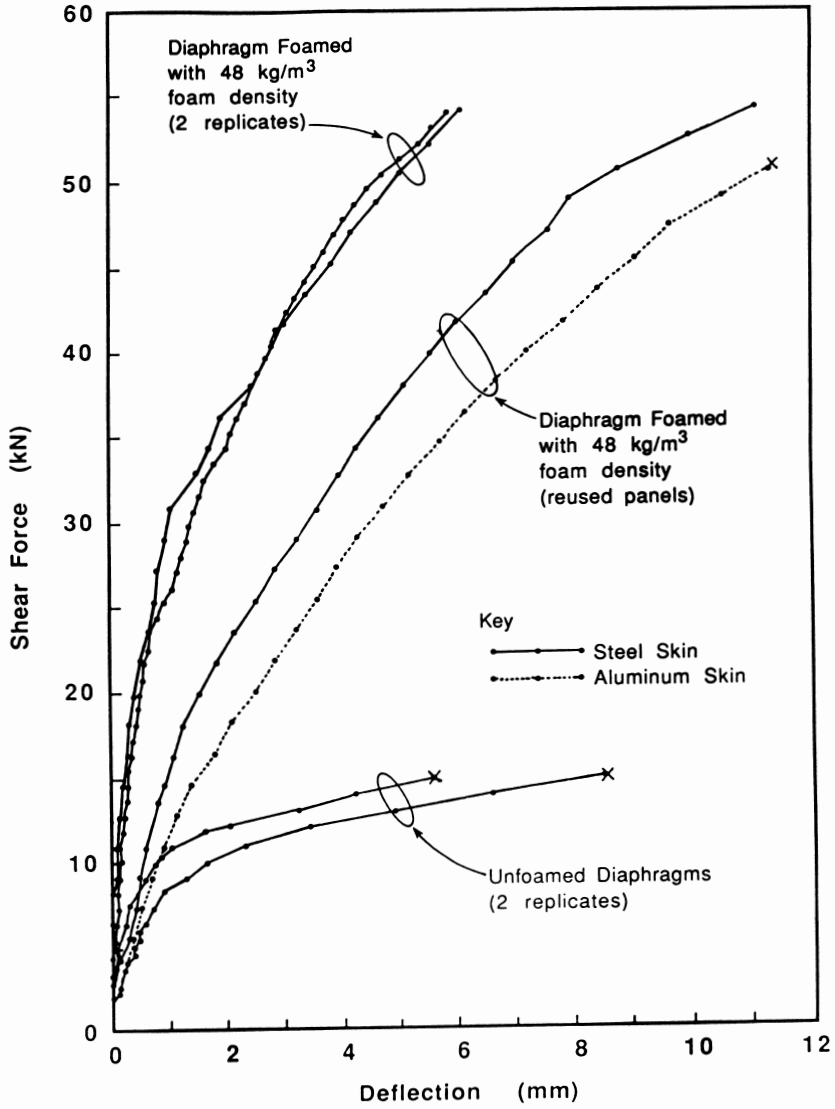

Figure 5. Load-deflection relationships for 2.44 m × 3.66-m diaphragms tested as cantilever. Note: plots marked with "x" at their ends were tested to failure and those without "x" were not tested to failure.

deflection plots are shown in Fig. 5. The first two shear tests were used to tune the testing apparatus and procedures, thus, the results of these two tests are not included in the summary Table or Fig. 5.

The load-deflection characteristics exhibited a nonlinear relationship, and duplicate pairs of experiments confirmed the repeatability of test results. The testing of diaphragms fabricated of steel skin and urethane foam in shear mode was not carried to failure. The test was stopped at 53.4 kN load due to limitation of load-cell capacity. Thus, the reported strength values of these diaphragms (Table II) do not represent their ultimate strength. The plots marked with "x" at their ends rep-

Table II. Load-deflection characteristics and failure modes of diaphragms tested in shear mode†

Type of sheathing	Foam density (kg/m³)	P_u (kN)	Δ (mm)	Strength (P_u/Δ) (kN/mm)	Failure mode
Steel	No foam	14.2	8.5	1.7	Skin buckling
Steel	No foam	14.3	5.6	2.6	Skin buckling
Steel	48	53.4	5.9	9.1	No failure‡
Steel	48	53.4	6.1	8.8	No failure‡
Steel§	48	53.4	11.2	4.8	No failure‡
Aluminum§	48	49.8	11.5	4.3	Shear failure in foam

†Diaphragms were 2.44 m × 3.66 m.
‡No failure occurred at the load shown. Testing was stopped because of limitation of load-cell capacity.
§Diaphragms cut out from the center (unfailed) area of larger systems initially tested as deep beams.

resent diaphragms tested to failure and plots without "x" represent diaphragms not tested to failure (Fig. 5).

To compare the strength of foamed and unfoamed diaphragms, duplicate pairs of unfoamed diaphragms with steel skin were built and tested in shear mode. The average shear strength of the unfoamed diaphragms was four times lower than that of their foamed counterparts (note that the foamed diaphragms were not tested to failure for the load specified in Table II). The unfoamed diaphragms exhibited an accordion-type sheet buckling deformation. Up to six major ripples were formed which originated at the diaphragm ends and gradually propagated towards the center. A similar mode of failure was observed when diaphragms were tested as deep beams.

Two 2.44 m × 3.66 m sections cut out from the center (unfailed) area of two 2.44 m × 6.10 m diaphragms, initially tested as deep beams, were tested in shear mode. As noted previously, when the larger diaphragms were tested as deep beams, failure was by shear in the foam at the sidelap joints, the reason for cutting off the first and last 1.22-m sections. The shear strength of these (used) systems was about 50% lower than that of the (unused) diaphragms tested in shear mode the first time. This reduction must be due to some "softening" effect of the foam as a result of repeated loading.

METHODS FOR CALCULATING SHEAR STIFFNESS

To calculate shear stiffness of diaphragms, it is necessary to separate the bending and shear deflections. The former can be calculated in standard ways; test information on the specific diaphragm is needed for the latter. The stiffness of a shear diaphragm is defined as the slope of the load-deflection curve in the nearly linear region below approximately 0.4 of the ultimate load (P_u) (Luttrell 1967; White 1978). The shear deflection for the load of (0.4* P_u) can be computed as

$$\Delta_s' = \Delta' - \Delta_b' \tag{3}$$

where:

Δ_s' = shear deflection for the load of ($0.4*P_u$),
Δ' = deflection obtained from the load-deflection curve for the load of ($0.4*P_u$),
Δ_b' = computed bending deflection at the free end of the cantilever beam diaphragm or at mid-span of the simple beam diaphragm.

Δ_b' is calculated as:

$$\text{Cantilever test } \Delta_b' = \frac{Pa^3}{3EI} \tag{4a}$$

$$\text{Simple beam test } \Delta_b' = \frac{63Pa^3}{8EI} \tag{4b}$$

where:

P = (0.4* P_u),
E = modulus of elasticity of perimeter member and of a beam element,
I = moment of inertia considering only the perimeter members of the test frame = $2A(b/2)^2$,
A = cross-sectional area of perimeter member.

Finally, the shear stiffness, G', of the diaphragm can be computed as

$$G' = \frac{0.4*P_u}{\Delta_s'}\left(\frac{a}{b}\right) \tag{5}$$

In Eq. 4, it is assumed that the bending moment is carried entirely by the perimeter members acting as flanges and the shear force alone is carried by the diaphragm web. In substance, any diaphragm system, including that of a cantilever test set-up, represents a plate girder in which two perimeter members constitute the flanges and the diaphragm constitutes the web.

For many panel configurations, the shear stiffness, G', varies with diaphragm length (Luttrell 1967). Much of the shear deflection is produced by imperfect connections of the shear diaphragm to the edge members, particularly at the ends of the panels. As the diaphragm is made longer, the end deflections have less influence on the total deflection. Hence, shear stiffness for a diaphragm increases with length.

It should be noted that in the test specimens, the metal siding was oriented parallel to the chords consistent with the way it would be oriented in the field for walls but perpendicular to the way it would be oriented for ceilings. A study by Davies and Bryan (1982) adjusts the stiffness of a diaphragm with the load applied parallel to the corrugation to that of a similar diaphragm with the load applied perpendicular to the corrugation by the equation

$$G_2' = (a/b)^2\, G_1' \tag{6}$$

where:

G_1' = shear stiffness of diaphragm with load applied parallel to the corrugation,
G_2' = shear stiffness of diaphragm with load applied perpendicular to the corrugation,
a,b = dimensions of the test frame shown in Fig. 1a and 1b.

Equation 6 is valid only when all components of the diaphragms compared are identical. Other adjustments, such as conversion of diaphragm stiffness test data for a given diaphragm length or metal thickness to other identically fabricated diaphragms but of different lengths or thickness can be made using equa-

tions given by Luttrell (1967) and Luttrell and Ellifritt (1970), respectively.

DESIGN RECOMMENDATIONS IN THE APPLICATION OF FOAM INSULATED METAL SKIN PANELS

Based on the load-deflection characteristics and failure modes observed, the following design factors can be suggested in the application of foam-insulated metal skin panels:

- Shear failure of stitch screws is undesirable because it occurs suddenly and is progressive. A more rigid interpanel connection, such as by increasing the number of stitch screws would improve performance.
- From a design standpoint, sheet tearing at the sidelap joints or at the sheet/purlin fasteners is perferable to shear failure of stitch screws because it insures that large deformations can take place without significant reduction in the collapse load.
- For thinner-gage metal panels, local and overall buckling of the cladding may be more critical than sheet tearing.
- Fatigue and environmental conditions not encountered in the laboratory testing should be taken into account in design application of foamed stressed-skin diaphragms. For example, it is not known what effect in-service conditions may have on the tightness of screw connections, nor how the foam would react with time. All types of foam undergo a significant degree of strain creep under sustained long-term loads (Ting 1986). Therefore, for roof application with long-term snow load condition, it is important to consider the shear creep behavior of the foam in the engineering analysis of the system.
- All possible modes of potential failure must be checked to determine the design strength of diaphragms. It is highly desirable that the final design should ensure a ductile failure.

CONCLUSIONS

The following conclusions may be stated on the basis of the work described:

1. A testing, control and computerized data acquisition system was developed for diaphragms simulating ceilings as deep beams and cantilever-type.
2. The load-deflection characteristics of the diaphragms tested were nonlinear. The connections seem to be the source of the non-linearity.
3. The sidelap seams were the weakest link of the diaphragms tested.
4. The combined action of urethane foam and metal skin provided high stiffness and strength for timber framed diaphragms. Strength of diaphragms increased by over three times when 32 kg/m^3 density foam was applied at the cavities between chords, and by over seven times when 48 kg/m^3 was applied. Strength is defined as the ultimate load per unit deflection.
5. The mode of failure of the unfoamed diaphragms was progressive and that of the foamed diaphragms was sudden and dramatic. Unfoamed diaphragms failed by mild sheet tearing at the sidelap joints and diaphragm ends, coupled with popping out of stitch screws and withdrawal of end fasteners. Foamed diaphragms failed in shear in the foam at the first sidelap joint, followed by mild sheet tearing at the same location.
6. Unfoamed diaphragms exhibited accordion-type sheet buckling deformations when tested as deep beams or as cantilevers. The deformations originated at the diaphragm ends and gradually propagated toward the center.
7. To apply the results reported in this study in design, the unknown effects of in-service environmental conditions and the potential changes of foam properties with time must be considered.

ACKNOWLEDGMENTS

FABRAL-Alcan Building Products Division of Alcan Aluminum Corporation, Lancaster, Pa. provided all the panels and fasteners. Sunseal Systems, Inc., Wayland, N.Y. provided the urethane foam as well as the foaming service. The authors appreciate this support.

REFERENCES

DAVIES, J. M. and E. R. BRYAN. 1982. Manual of stressed skin diaphragm design. John Wiley and Sons, Inc., New York. pp. 441.

GEBREMEDHIN, K. G. and W. W. IRISH. 1986. Ultimate load-deflection characteristics and failure modes of ceiling diaphragms for farm buildings. Wood Fiber Sci. 18(4): 565–578.

HOAGLAND, R. C. and D. S. BUNDY. 1983. Strength and stiffness of screw-fastened roof panels for pole buildings. Trans. of ASAE (Am. Soc. Agr. Eng.) 2b(2): 512–515.

LUTTRELL, L. D. 1967. Strength and behavior of light-gauge steel shear diaphragm. Cornell Research Bulletin 67-1. pp. 41.

LUTTRELL, L. D. and D. S. ELLIFRITT. 1970. The strength and stiffness of steel deck subjected to in-plane loading. Report No. 2011 and Supplement, Steel Deck Institute, Canton, Ohio.

TING, Raymond, M. L. 1986. Structural properties of factory insulated panels. Metal Architecture. March 1986.

TURNBULL, J. E., K. C. McMARTIN, and A. T. QUAILE. 1982. Structural performance of plywood and steel diaphragms. Can. Agric. Eng. 24: 135–140.

TURNBULL, J. E., J. A. THOMPSON, and A. T. QUAILE. 1985. Steel roof diaphragms for wind bracing in agricultural buildings. Can. Agric. Eng. 28(2): 155–165.

WHITE, R. N. 1978. Diaphragm action of aluminum-clad timber-framed buildings. ASAE Paper No. 78–4501, Am. Soc. Agr. Eng., St. Joseph, Mich. pp. 36.